communications medicine

Article

https://doi.org/10.1038/s43856-024-00570-3

Jointly estimating epidemiological dynamics of Covid-19 from case and wastewater data in Aotearoa New Zealand

Check for updates

Leighton M. Watson [1] ✉, Michael J. Plank [1], Bridget A. Armstrong[2], Joanne R. Chapman[2], Joanne Hewitt[2], Helen Morris [2], Alvaro Orsi[2], Michael Bunce[2], Christl A. Donnelly [3,4] & Nicholas Steyn[3]

Abstract

Background Timely and informed public health responses to infectious diseases such as COVID-19 necessitate reliable information about infection dynamics. The case ascertainment rate (CAR), the proportion of infections that are reported as cases, is typically much less than one and varies with testing practices and behaviours, making reported cases unreliable as the sole source of data. The concentration of viral RNA in wastewater samples provides an alternate measure of infection prevalence that is not affected by clinical testing, healthcare-seeking behaviour or access to care.

Methods We construct a state-space model with observed data of levels of SARS-CoV-2 in wastewater and reported case incidence and estimate the hidden states of the effective reproduction number, *R*, and CAR using sequential Monte Carlo methods.

Results We analyse data from 1 January 2022 to 31 March 2023 from Aotearoa New Zealand. Our model estimates that *R* peaks at 2.76 (95% CrI 2.20, 3.83) around 18 February 2022 and the CAR peaks around 12 March 2022. We calculate that New Zealand's second Omicron wave in July 2022 is similar in size to the first, despite fewer reported cases. We estimate that the CAR in the BA.5 Omicron wave in July 2022 is approximately 50% lower than in the BA.1/BA.2 Omicron wave in March 2022.

Conclusions Estimating *R*, CAR, and cumulative number of infections provides useful information for planning public health responses and understanding the state of immunity in the population. This model is a useful disease surveillance tool, improving situational awareness of infectious disease dynamics in real-time.

Plain language summary

To make informed public health decisions about infectious diseases, it is important to understand the number of infections in the community. Reported cases, however, underestimate the number of infections and the degree of underestimation likely changes with time. Wastewater data provides an alternative data source that does not depend on testing practices. Here, we combined wastewater observations of SARS-CoV-2 with reported cases to estimate the reproduction number (how quickly infections are increasing or decreasing) and the case ascertainment rate (the fraction of infections reported as cases). We apply the model to Aotearoa New Zealand and demonstrate that the second wave of infections in July 2022 had approximately the same number of infections as the first wave in March 2022 despite reported cases being 50% lower.

Understanding and predicting the trajectory of infectious diseases is important in planning an effective public health response. Reported case data depend heavily on testing modalities and practices which typically change over time, resulting in considerable uncertainty in the case ascertainment rate (CAR; the fraction of infections that are officially reported). During the COVID-19 pandemic, many countries relied primarily on symptom-based testing programs to inform situational awareness and public health responses. In Aotearoa New Zealand, the CAR for COVID-19 has been influenced by factors such as access to testing, a shift from healthcare worker-administered polymerase chain reaction (PCR) tests to self-administered rapid antigen tests (RATs), reduction in rates of symptomatic and severe disease due to rising population immunity, relaxation of testing requirements and recommendations, and/or lack of perceived need to test or 'pandemic fatigue'[1–3]. As a result, over time, officially reported cases of COVID-19 have become a less reliable measure of levels of SARS-CoV-2 infection.

Data on hospital admissions and deaths are more consistent and are less affected by testing practices and behavioural change than reported cases but are subject to additional delays[4] that limit their usefulness for understanding disease dynamics. Infection prevalence surveys[5] that aim to regularly test a representative sample of the population are the gold standard for tracking the spread of infectious disease, but these surveys are resource-

[1]School of Mathematics and Statistics, University of Canterbury, Christchurch, New Zealand. [2]Institute of Environmental Science and Research Ltd, Porirua, New Zealand. [3]Department of Statistics, University of Oxford, Oxford, United Kingdom. [4]Pandemic Sciences Institute, University of Oxford, Oxford, United Kingdom. ✉e-mail: leighton.watson@canterbury.ac.nz

intensive, making them harder to justify as countries move out of the acute phase of the pandemic. The UK was the only country to implement regular representative national SARS-CoV-2 prevalence surveys[6,7], and there are no current plans for similar surveys in New Zealand.

Wastewater surveillance, where levels of SARS-CoV-2 RNA in wastewater samples are measured, can provide additional data on the prevalence of the virus that are unaffected by individual testing and self-reporting behaviours. Wastewater surveillance (also known as wastewater-based epidemiology or WBE) also has the potential to contribute to an integrated global network for disease surveillance[8–10]. These data, however, can be highly variable and subject to other biases, such as rainwater dilution, sampling methodologies, and changing locations of selected sampling sites. To realise this potential, appropriate models and analytical tools are needed to deliver epidemiological insights from raw data.

Two previous studies have presented novel methodologies for the real-time estimation of the effective reproduction number using wastewater data[11,12], while others have leveraged or extended these methods[13–16]. One study used reported cases to estimate the reproduction number and then fitted a model to estimate this quantity from wastewater data[17]. Another study used wastewater data to fit a mathematical model of multiple viral strains[18] from which estimates of the reproduction number can be derived. Other studies have analysed wastewater data but did not use it to estimate the reproduction number[19,20]. Only[11] presented a model for simultaneously considering clinical and wastewater data, however they assume a fixed ascertainment rate. No previous work has combined wastewater-based epidemiology with reported cases to infer changes in case ascertainment over time.

Semi-mechanistic models based on the renewal equation are a popular method for epidemic forecasting and estimation of the instantaneous reproduction number[21–23]. Such methods are robust to constant under-ascertainment of cases, but may be biased by rapid changes in CAR and cannot provide any information about the total number of infections. In this paper, we extend the renewal equation framework[21–23] for reproduction number estimation to incorporate wastewater time-series data. The model treats the instantaneous reproduction number and CAR as hidden states and reported cases and quantity of viral RNA in wastewater as observed states. We use a sequential Monte Carlo approach to infer the hidden states. We apply the model to national data from Aotearoa New Zealand on reported COVID-19 cases and the average number of SARS-CoV-2 genome copies per person per day measured in municipal wastewater samples between January 2022 and March 2023. Because the relationship between infections and wastewater concentration is only determined in the model up to an overall scaling constant, it cannot be used to infer the absolute CAR but can be used to estimate relative changes in case ascertainment over time. The model is designed to be regularly updated as new data become available, producing real-time estimates of the effective reproduction number and relative change in CAR. The model has been used to support situational awareness via regular reports to the New Zealand Ministry of Health from November 2022 to date.

From March 2020 until December 2021 New Zealand used strict border controls and intermittent non-pharmaceutical interventions to suppress and eliminate transmission of SARS-CoV-2. By the beginning of 2022, there had been a cumulative total of around three confirmed cases of COVID-19 per 1000 people and around 90% of the population over 12 years old had received at least two doses of the Pfizer-BioNTech vaccine. From October 2021, interventions were progressively eased, and in January 2022, the B.1.1.529 (Omicron) variant began to spread in the community, causing the first large wave of infection. Since then community transmission has been sustained, with multiple further waves of infection being driven by various Omicron subvariants. Between 1 January 2022 and 31 March 2023, there was a cumulative total of around 440 confirmed cases per 1,000 people, most of which were from self-administered RATs. During this period, SARS-CoV-2 concentration was regularly measured at various wastewater treatment plants, providing an additional data source on changes in community prevalence over time.

We model the epidemic dynamics and the observed case and wastewater data at the national level, aggregating over New Zealand's population of 5.1 million and ignoring regional variations. This is similar to other studies that have aggregated regional case and/or wastewater data to produce national-level estimates in countries with a comparable population size[24–26]. Our methodology could, in principle, be applied at a finer geographical scale, although this would come at the cost of higher levels of noise.

Methods

Data

National daily reported cases of COVID-19 were obtained from the New Zealand Ministry of Health[27]. Until February 2022, these cases were diagnosed solely by healthcare-administered PCR testing. From February 2022, in response to the rapid increase in reported cases, RATs were widely distributed. Since then, the vast majority of reported cases have been from self-administered RATs, with results reported via an online portal. Hence, data on the number of tests conducted are not available. Reported cases are shown in Fig. 1. As these data exhibit a clear day-of-the-week effect, we remove the weekly trend before fitting the model (see Supplementary Material Section 1.2 for details).

SARS-CoV-2 concentration data from wastewater samples tested by the Institute for Environmental Science and Research (ESR) were used for this study[28]. Wastewater samples were collected every week at municipal wastewater treatment plants located throughout the country, serving communities with populations ranging from 400 to over 500,000 people. Typically 70–90% of the national population connected to reticulated wastewater was covered by wastewater sampling in any given week (60–124 sites, usually sampled twice per week). Each site-level measurement was normalised to provide an estimate of the number of genome copies per person per day for that site (see Supplementary Material Section 1.1). Typically multiple sites were sampled per day and, for each day that had at least one sample, we calculated the catchment-population-weighted average of the genome copies per person (see Fig. 1). Because we do not attempt to model regional variations, we assumed this provided a series of representative observations of the average concentration of genomic material in the national wastewater.

Hidden state model

We construct a state-space model (Fig. 2) consisting of time-varying hidden states (the instantaneous reproduction number R_t, daily case ascertainment rate CAR_t, and daily infection incidence I_t) and time-varying observed states (daily reported cases of COVID-19 C_t and daily wastewater observations W_t)[29]. We use subscript $s{:}t$ to refer to all values between day s and t inclusive.

We assume the hidden states R_t and CAR_t follow independent Gaussian random walks, encoding the fact we expect them to vary continuously over time. We also assume that the hidden state I_t follows a Poisson renewal process, a simple epidemic model commonly used when estimating R_t[21]. Thus our state-space transitions are governed by:

$$(R_t|R_{t-1}) \sim N_{(0,\infty)}(R_{t-1}, \sigma_R R_{t-1}) \tag{1}$$

$$(CAR_t|CAR_{t-1}) \sim N_{(0,1)}(CAR_{t-1}, \sigma_{CAR}) \tag{2}$$

$$(I_t|R_t, I_{1:t-1}) \sim Poisson\left(R_t \sum_{u=1}^{t-1} g_u I_{t-u}\right) \tag{3}$$

Parameters σ_R and σ_{CAR} determine how quickly R_t and CAR_t vary. The standard deviation of the transition distribution for $R_t \to R_{t+1}$ is given by $\sigma_R R_t$, which means that R_t varies more rapidly at larger values. The distribution for R_t was truncated on $(0, \infty)$ and for CAR_t on $(0, 1)$. Finally, g_u is

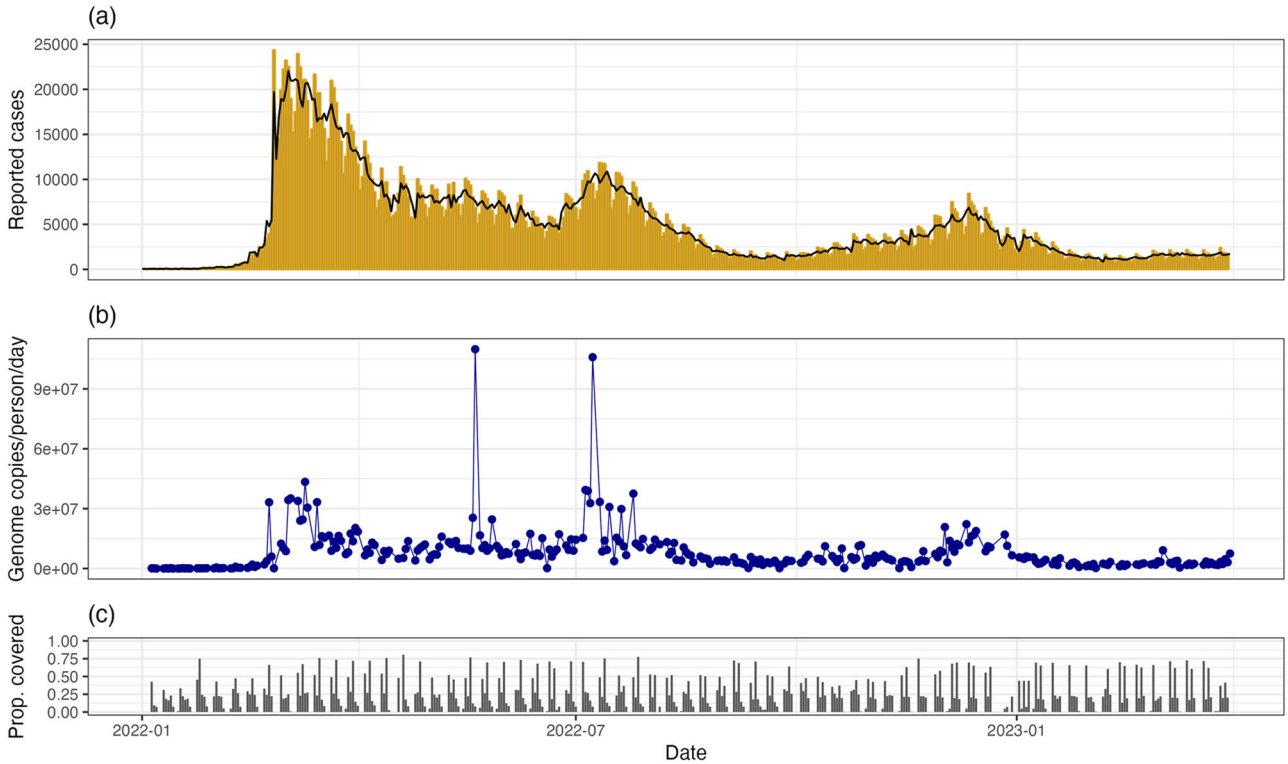

Fig. 1 | Reported daily cases and wastewater data between 1 January 2022 and 31 March 2023 in Aotearoa New Zealand. a Reported daily cases of COVID-19. The black line shows the adjusted case series with the multiplicative day-of-the-week effect removed (see Supplementary Material Section 1.2). **b** SARS-CoV-2 genome copies per person per day in sampled wastewater. The two outliers in wastewater data arise from estimates of a high wastewater flow rate in Wellington following high rainfall. Since rainfall is a source of noise in wastewater sampling, we retain these samples in our analysis. **c** Proportion of the total population covered by sampled wastewater catchments. Reported case data were obtained from the New Zealand Ministry of Health[27] and wastewater data were obtained from ESR[28].

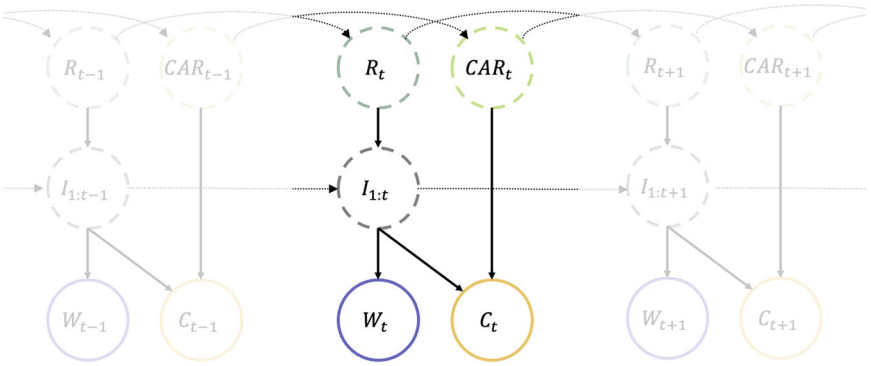

Fig. 2 | Diagram of the state-space model. Schematic of the model showing the dependency between hidden-states (dashed circles) and the observed data (solid circles). R_t is the instantaneous reproduction number on day t, CAR_t is the case ascertainment rate on day t, I_t is the number of new infections on day t, C_t is the number of reported cases on day t, and W_t is the observed wastewater, measured as the total genome copies per person per day for the sites that were sampled on day t. $I_{1:t}$ denotes the set of states $\{I_1, I_2, \ldots, I_t\}$. In practice, the current infections I_t, reported cases C_t and wastewater W_t depend only on recent values of I_t as specified by the generation interval distribution, the infection-to-reporting distribution, and infection-to-shedding distribution, respectively (see Methods).

the pre-determined generation time distribution, describing the proportion of transmission events that occur u days after infection (see Supplementary Material Section 2.7).

We assume that the expected number of reported cases μ_t^c at time t is equal to CAR_t multiplied by the convolution of past infections with the infection-to-reporting distribution L_u:

$$\mu_t^c = CAR_t \sum_{u=1}^{t} I_{t-u} L_u \tag{4}$$

Similarly, we assume that the expected number of genome copies μ_t^w detected per person at time t is equal to the convolution of past infections with the infection-to-shedding distribution ω_u, multiplied by a fixed parameter α representing the average total detectable genome copies shed into the wastewater by an infectious individual, divided by total national population size N:

$$\mu_t^w = \frac{\alpha}{N} \sum_{u=1}^{t} I_{t-u} \omega_u \tag{5}$$

We model reported cases using a negative binomial distribution:

$$(C_t | CAR_t, I_{1:t}) \sim NegBin\left(r = k_c, p = \frac{k_c}{k_c + \mu_t^c}\right) \tag{6}$$

Table 1 | Parameter values used in the model

Parameter	Symbol	Value
Coefficient of variation of R_t transitions	σ_R	Fitted
Std dev. of CAR_t transitions	σ_{CAR}	Fitted
Reported cases tuning parameter	k_c	Fitted
Wastewater tuning parameter	k_w	Fitted
Generation time distribution[52,53]	g_u	Mean = 3.3 days, s.d. = 1.3 days
Infection-to-reporting distribution	L_u	Mean = 5.8 days, s.d. = 2.6 days
Infection-to-shedding distribution	ω_u	Mean = 5.2 days, s.d. = 2.9 days
Average total genome copies per infection	α	3×10^9 [2×10^9, 4×10^9]
Fixed-lag resampling window	h	30 days

The infection-to-reporting and infection-to-shedding distributions are calculated as convolutions of the incubation period distribution[34] and the onset-to-reporting and onset-to-shedding distribution[35] respectively (see Supplementary Material Section 2.7).

which has mean μ_t^c and variance $\mu_t^c\left(1+\frac{\mu_t^c}{k_c}\right)$. A negative binomial distribution is used to account for noise in the observations beyond that predicted by a binomial distribution. This is a common choice in other methods of reproduction number estimation[23,30].

The observed wastewater data W_t is the total genome copies per person from the wastewater sites sampled on day t. We model this using a shape-scale gamma distribution:

$$(W_t|I_{1:t}) \sim \begin{cases} \Gamma\left(k_w \mathrm{pop}_t, \frac{\mu_t^w}{k_w \mathrm{pop}_t}\right) & \text{if } \mathrm{pop}_t > 0 \\ \mathcal{I}(W_t = 0) & \text{if } \mathrm{pop}_t = 0 \end{cases} \quad (7)$$

which has mean μ_t^w and variance $\frac{(\mu_t^w)^2}{k_w \mathrm{pop}_t}$. This assumes that the observed daily data are independent draws from the national distribution, which may not hold if there are regional differences between the subsets of sites that are sampled on different days. In practice, any such differences will be absorbed into the variance of the daily observation distribution via fitting of the dispersion parameter k_w. Since we marginalise out the effect of this parameter when presenting results, the increased uncertainty associated with regional variability is propagated through to the credible intervals. The variable pop_t refers to the total population in the catchment areas of the sampled wastewater sites on day t. Setting the variance of the observation distribution to be inversely proportional to pop_t allows the model to account for increased variability around the national mean on days when fewer or smaller sites were sampled. $\mathcal{I}$ is the indicator function, so on days when no sites were sampled, the probability of observing no wastewater samples is set to 1, and the model fits to case data alone.

Consistent with previous models[31,32], this formulation assumes that the expected population shedding rate is proportional to the number of infected individuals, with observations drawn from a distribution around this mean. We used a gamma distribution, which is a reasonably flexible choice for a non-negative continuous random variable. However other distributions could be considered, such as a Weibull or log-normal.

In the absence of additional information, we are unable to estimate α, which is proportional to the average total genome copies shed by an infected individual over the course of their infection. This means we are unable to estimate the absolute value of CAR_t. Instead, we run the model with a range of different values for α, and estimate the change in CAR_t relative to its initial value. This additionally requires the assumption that α is constant over time, which is unlikely to be true in general and is a key limitation of our model (see Discussion).

In practice, the range of values of α that we used (see Table 1) was chosen by calibrating model output for the number of infections with external sources of information. Firstly, we compared model output to the number of cases in a cohort of around 20,000 border workers who were tested weekly between January and July 2022[33]. Secondly, around 40% of all 20–25-year-olds (an age group unlikely to have a higher CAR than older adults) reported a case of COVID-19 in the 6 months from 1 February to 31 July 2022[27]. This suggests that the overall CAR for this period was likely to be at least 0.4, which translates to an approximate upper bound of 4 million for the total cumulative number of infections up to 31 July 2022. Neither of these observations definitively determines the number of infections as they are subject to approximation, bias and uncertainty, but they nevertheless serve to bracket the likely range of values for the parameter α.

The infection-to-reporting and infection-to-shedding distributions are calculated as the convolution of the incubation period distribution with the onset-to-reporting and onset-to-shedding distribution respectively. The incubation period is modelled as a Weibull distribution with a mean of 2.9 days and a standard deviation of 2.0 days[34]. The onset-to-reporting distribution is estimated empirically from New Zealand case data extracted on 16 September 2022, representing over 1.2 million cases, and has a mean of 1.8 days and a standard deviation of 1.8 days. The onset-to-shedding distribution comes from ref. 35 and has a mean of 0.7 days and a standard deviation of 2.6 days. The resulting infection-to-reporting distribution has a mean of 5.8 days and a standard deviation of 2.6, and the resulting infection-to-shedding distribution has a mean of 5.2 days and a standard deviation of 2.9 days (see Supplementary Fig. 1).

The model is solved using a bootstrap filter[36] with fixed-lag resampling. This produces estimates for the marginal posterior distribution of the hidden states at each time step. The random walk step variance parameters (σ_R and σ_{CAR}) and observation variance parameters (k_c and k_w) are estimated using a particle marginal Metropolis-Hastings Markov chain Monte Carlo method. We use an uninformative uniform prior distributions for these parameters, with the exception of σ_{CAR}, where we use an informative prior distribution to ensure an appropriate level of smoothness in our estimates of CAR_t. Different parameter values are fitted in three-month blocks to allow for some variation over time. See Supplementary Material Section 2 for further details of the numerical method.

Reporting summary

Further information on research design is available in the Nature Portfolio Reporting Summary linked to this article.

Results

Reproduction number, relative case ascertainment, and infection incidence

The estimated value of the reproduction number R_t (Fig. 3a) increases from around 1 at the beginning of 2022 to a peak of 2.46 (95% CrI 2.04, 3.20) on 18 February 2022 (95% CrI 10 Feb, 23 Feb), corresponding to the sharp increase in cases seen during the first Omicron wave, which was a mixture of the BA.1 and BA.2 variants[37]. The estimated value of R_t drops below 1 on 1

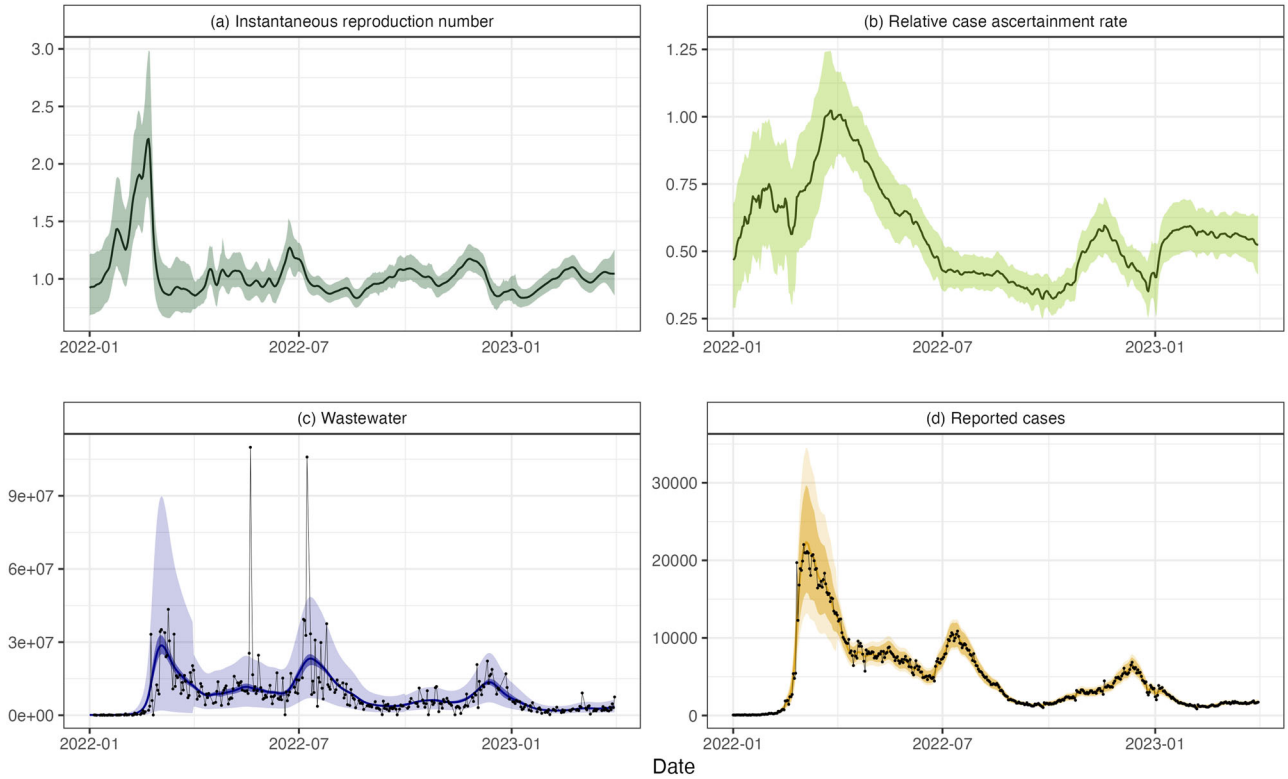

Fig. 3 | Results for Aotearoa New Zealand data from 1 January 2022 to 31 March 2023. a Instantaneous reproduction number R_t, **b** relative case ascertainment rate (compared to the central estimate on 1 April 2022), **c** wastewater data W_t measured in genome copies per person per day and **d** reported cases C_t. Results assume the average total shedding per infection does not vary over time ($\alpha = 3 \times 10^9$). Solid lines present central estimates. Shaded regions show 95% credible intervals on the value of the hidden states (subplots a and b) and 95% credible intervals on the expected reported cases and wastewater data (darker shaded regions in subplots c and d) and 95% credible intervals on the prediction distribution for wastewater data and reported cases (lighter shaded regions in subplots c and d). Black dots show the observed data.

March 2022 (95% CrI 25 Feb, 5 Mar) and infection incidence peaked on 28 February 2022 (95% CrI 23 Feb, 7 Mar), suggesting this is when the wave peaked.

The estimated CAR (Fig. 3b) increases rapidly between mid-February and mid-March 2022. RATs became widely available for the first time in the last week of February 2022. This likely led to a substantial increase in case ascertainment as the testing system, which had previously relied solely on laboratory-processed PCR tests, had become overwhelmed[3]. The estimated CAR approximately halves between April and July 2022, when a second wave of infection caused by the BA.5 Omicron subvariant[33,37] occurred. This second wave was visible in both reported cases and wastewater sampling, with estimated peak infections occurring on 7 July 2022 (95% CrI 3 Jul, 12 Jul). The estimated CAR increases somewhat between mid-2022 and early 2023, with a noticeable dip in December 2022, possibly reflecting reduced testing during the Christmas and summer school holiday period (from mid-December to late-January/early-February). Alternatively, the estimated increase in CAR from mid-2022 could be explained by a decrease in the average genome copies shed by an infected individual α, although without further information we are unable to discern changes in α. Overall, the model provides a reasonably good fit to the observed data on cases and wastewater (Fig. 3c, d).

Figure 4a, b shows the estimated daily incidence and cumulative infections for three values of α, corresponding to estimated CAR values on 1 April 2022 of 0.42 (95% CrI 0.35, 0.50), 0.61 (95% CrI. 0.51, 0.71), and 0.80 (95% CrI. 0.67, 0.93), for $\alpha = 2 \times 10^9$, 3×10^9 and 4×10^9, respectively. For comparison, the graphs also show the number of cases per capita in a cohort of approximately 20,000 border workers who were tested weekly between January and July 2022[33], scaled according to population size. These data were used to help inform the range of values of α selected (see Methods).

Whilst peak reported cases (adjusted for the day-of-the-week effect) in the second wave were only 49% of the peak in the first wave (10,879 vs 22,038 respectively), under the assumption of constant α, the central estimate from the model suggests that true infections peaked at approximately 78% of the peak of the initial wave (Fig. 4a). Figure 4c–e shows the estimated absolute and relative CAR and R. These panels show that, while we are uncertain about the absolute level of infections and CAR, the relative CAR and reproduction number estimates are robust to reasonable choices for (constant) α.

Fitting the model to case data alone instead of cases and wastewater (see Supplementary Fig. 7) produced qualitatively similar estimates of R_t, but with greater temporal fluctuations. Fitting the model to wastewater data alone led to substantially wider credible intervals, although the overall trend was similar. Estimates of the relative CAR are only possible when fitting to case and wastewater data simultaneously.

Parameter estimates

The estimated standard deviation σ_R of the random walk on R_t was greatest in the first time period (1 Jan – 31 Mar 2022)—see Table 2. This is unsurprising as it coincided with the rapid increase and then decrease in incidence associated with the first Omicron wave. σ_R decreased in the second period (1 Apr–30 Jun 2022) and then remained relatively constant throughout the remaining periods (1 Jul 2022–31 Mar 2023). The estimated standard deviation σ_{CAR} of the random walk on CAR_t was also estimated to be greatest in the first time period, although this is primarily because we applied a prior distribution with a higher mean in this period (see Supplementary Material Section 2.5).

The estimated variance parameters, k_c and k_w, for cases and wastewater observations, were lowest in the first time period (1 Jan 2022–31 Mar 2022).

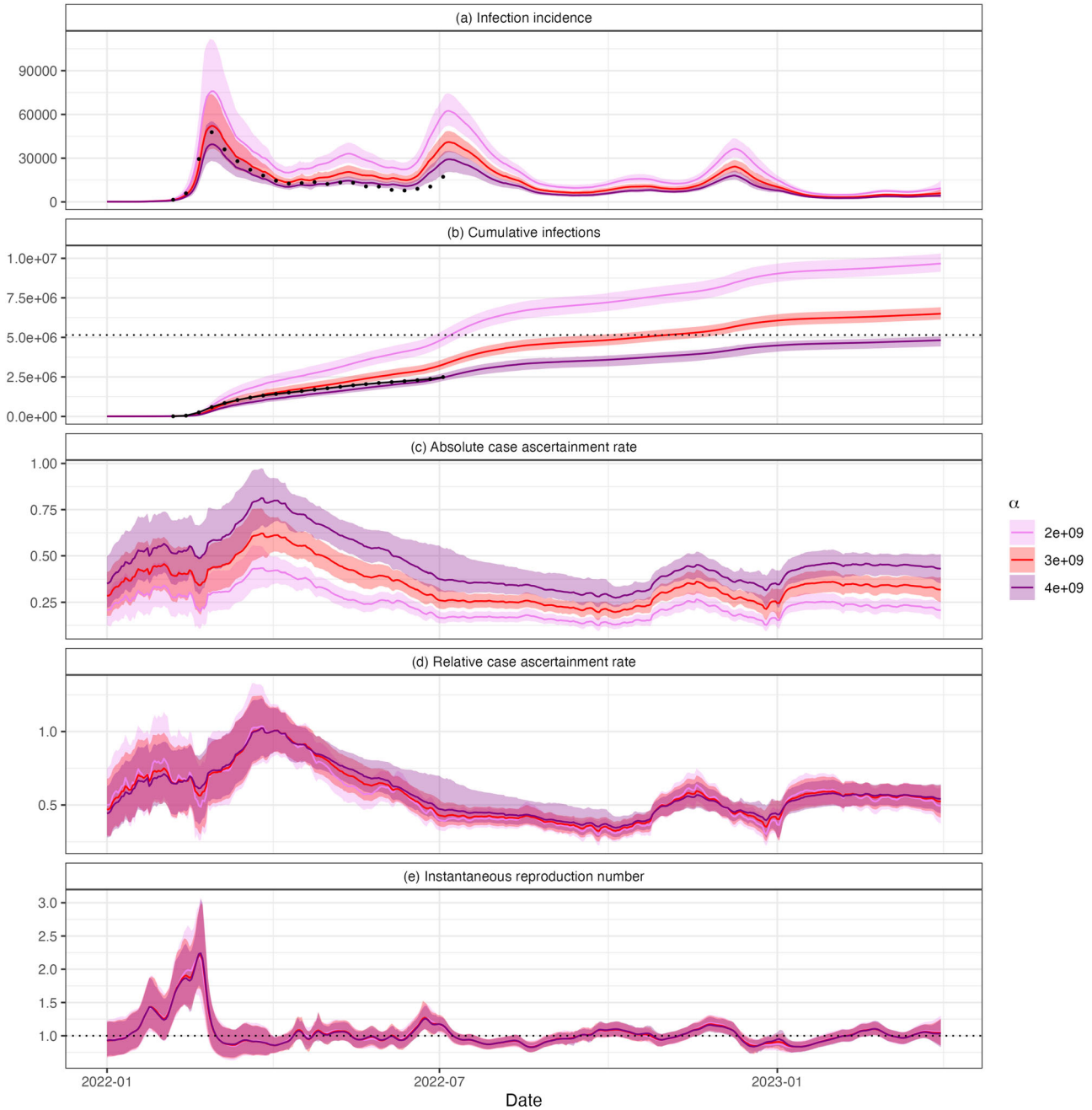

Fig. 4 | Sensitivity of results to the choice of *α*. Estimated **a** daily infections I_t, **b** cumulative infections $\sum_{s=0}^{t} I_s$, **c** case ascertainment rate CAR_t, **d** relative case ascertainment rate (compared to the central estimate on 1 April 2022) and **e** instantaneous reproduction number, R_t. Results are presented for three values of α: 2×10^9, 3×10^9 and 4×10^9. Solid lines show central estimates and coloured regions are the 95% CrIs. Estimates and credible intervals on cumulative infections are calculated by taking cumulative sums of the estimates and credible intervals in panel (**a**). Black dots in panels (**a**, **b**) show the number of per capita cases in a cohort of regularly tested border workers, scaled according to population size. The horizontal dashed black lie in panel (**b**) shows the New Zealand population at the end of 2022 (5.15 million people)[54]. While changing α results in different estimates of infections and absolute CAR, the relative CAR and reproduction number estimates are robust to different values, provided α remains relatively constant.

This implies there is more variability in the data that is not explained by the model in this time period, possibly as a consequence of the sharper variations in incidence compared to the later time periods. A less consistent weekly pattern in reported cases during the first time period, and higher levels of noise in wastewater observations at the low concentrations seen at the beginning of 2022, could also be contributing factors.

Discussion

Wastewater-based epidemiology has been used globally for COVID-19 surveillance and has been shown to be a useful public health tool for policy and public health responses[38]. We present a semi-mechanistic model that combines reported cases with wastewater data to estimate the time-varying reproduction number and CAR. This work demonstrates the value of wastewater-based epidemiology and how the additional data that it provides can be combined with traditional monitoring (e.g. reported cases) to learn more about the state of an epidemic, disease dynamics, and the true number of infections in the community. This provides useful information to inform the public health response.

To make reliable estimates of the state of the epidemic from reported cases, it is essential to understand how case ascertainment changes with

Table 2 | Central estimates and 95% credible intervals for estimated model parameters in each time period

Period starting	σ_R	σ_{CAR}	k_c	k_w(×10^{-6})
1 Jan 2022	0.12 (0.069, 0.21)	0.03 (0.017, 0.043)	31 (20, 49)	1.5 (1.1, 2.0)
1 Apr 2022	0.069 (0.041, 0.12)	0.0099 (0.0053, 0.014)	170 (100, 250)	4.8 (3.2, 6.8)
1 Jul 2022	0.037 (0.02, 0.066)	0.0063 (0.0018, 0.01)	330 (220, 400)	4.8 (3.3, 6.5)
1 Oct 2022	0.038 (0.02, 0.068)	0.011 (0.0073, 0.014)	170 (110, 270)	7.2 (4.7, 10.0)
1 Jan 2023	0.038 (0.018, 0.073)	0.0093 (0.0041, 0.015)	150 (84, 330)	6.8 (4.4, 10.0)

Dates in the 'Period' column are the start date for the three-month period. All outputs presented to 2 s.f. Higher values of σ_R and σ_{CAR} suggest R_t and CAR_t vary faster. Higher values of k_c and k_w indicate a lower variance in the corresponding observation distribution. Note a different prior distribution was used for σ_{CAR} in the first period (see Supplementary Material Section 2.5), which may also impact estimates of other parameters in this period.

time. For example, are there fewer cases because there are fewer infections or because fewer people are reporting? We apply our model to national data from Aotearoa New Zealand and derive insights into changes in case ascertainment that would not be possible using case data alone. Reported cases during the second wave in July 2022 were substantially lower than in the first wave in February and March 2022. However, the model infers that there was a substantial drop in case ascertainment between these waves, and the true number of infections was likely more similar in each wave. The reduced CAR during the second and subsequent waves may have been due to a higher number of reinfections with individuals displaying fewer symptoms or due to "pandemic fatigue" and reduced compliance with public health measures, including testing. This type of insight would not be possible without regular wastewater surveillance data and without a robust analytical framework in which to integrate these data with traditional epidemiological data streams.

We apply our model to the first period of widespread community transmission of SARS-CoV-2 in New Zealand. During this time, rapid antigen tests were freely available to everyone, there was a requirement to report positive results, and a mandatory isolation period for cases with financial support via employers. Partly as a result of these factors, the CAR, while lower than in the previous elimination phase, was still reasonably high. The mandatory isolation period was removed in September 2023, which led to a substantial drop in case ascertainment. For the datasets we consider, similar (albeit noisier) estimates for the reproduction number could be obtained from case data alone. However, in a context where case ascertainment is low and/or unrepresentative, wastewater data are likely to add even greater value compared to using reported cases. In contrast, in a low-prevalence context (e.g., pre-Omicron in New Zealand), the applicability of the method would be constrained by the amount of noise in the wastewater data. In this situation, wastewater surveillance may be better used for presence/absence monitoring, for example, as an early warning system for the presence of infection in specific catchments, as opposed to quantitative estimation[39].

Strengths of our model include the fact that it has relatively minimal data requirements, requiring only time series for reported cases and wastewater concentrations. The model can be fitted to datasets in which different sites are sampled on different days and some days have no observed data. This means that it could be readily applied in other jurisdictions with wastewater surveillance programs, either for SARS-CoV-2 or other pathogens such as influenza viruses[38,40]. It is a relatively simple model with minimal mechanistic assumptions and parsimonious parameterisation. This avoids the need for assumptions about time-varying contact patterns, transmission rates, and the level of prior immunity that are required by more complex mechanistic models. The model we present here was operationalised by ESR in late 2022, and results for R_t and relative CAR are regularly provided to the Ministry of Health to inform situational awareness and decision-making.

There are several limitations to this model and the results. We assume that the average number of genome copies shed by an infected individual (represented by the parameter α) was constant between January 2022 and March 2023 and did not depend on the infecting variant or history of prior infection or vaccination. It is possible that some of the inferred changes in CAR may be partly explained by these factors. For example, some of the inferred increase in case ascertainment between October and December 2022 may have been due to decreasing α, caused by a combination of new immune evasive subvariants displacing the previously dominant BA.5 variant[41] and/or an increase in the proportion of reinfections or asymptomatic infections[27]. Although estimates of viral shedding rates per infected individual are available[31,32], the value of α may also depend on the physical characteristics of the wastewater collection system, sample collection method, and the method used to quantify the concentration of SARS-CoV-2 RNA in samples. Therefore, α is likely to vary between jurisdictions and will require recalibration using local data.

As we are unable to estimate the true value of α, we are unable to estimate the absolute CAR. Nonetheless, relative CAR is a useful metric and, given an estimated range of values for α, we are able to provide plausible bounds on the total number of infections (Fig. 4).

Wastewater surveillance does not provide any information on how infections are distributed among population groups (e.g. age groups, ethnicity) and biases in self-administered testing mean that case counts are not representative either. This information is important for assessing the clinical burden of disease and addressing health inequities[42]. Thus, other approaches are needed to determine the distribution of disease burden, such as representative sampling[7,43], cohort studies[44] or sentinel surveillance[45,46]. Although wastewater surveillance could, in principle, be used to investigate differences in prevalence and case ascertainment between sites and/or regions, this would require adaptions to our method that are beyond the scope of this study.

As our model is flexible, future work could integrate hospitalisations (such as in ref. 47) and death data. In principle, this could allow the effects of varying CAR and varying rates of shedding per infection to be separated. However, this would additionally require the effects of age, immunity, ethnicity, and other variables on clinical severity to be accounted for.

Although national-level approaches to situational awareness and reproduction number estimation are common[25,48,49], particularly in countries such as New Zealand with relatively small population size, this ignores regional variations. Results should, therefore, be interpreted as national averages, which could mask demographic and spatial heterogeneity. Our model could be implemented at a regional level so that local epidemic dynamics can be compared, although this would be subject to increasing levels of noise in the wastewater data at finer spatial scales. This paper has focused on modelling for inference: understanding epidemic dynamics that have already occurred. However, the state-space transition model coupled with the estimated parameters provides a natural method for forecasting[23,50]. Forecasts generated using this state-space transition model naturally incorporate increasing uncertainty about the future reproduction number and CAR.

While this model focused on COVID-19, there is a wealth of genetic information within municipal wastewater that could also benefit from modelling. The detection and concentration of viral, bacterial and antimicrobial resistance genes within wastewater have the ability to inform public health decision-making in a number of ways, especially as methodology is refined allowing more rapid turnaround times. As many jurisdictions seek to retain the wastewater capabilities they built during the

pandemic phase of COVID-19 (and to diversify microbial targets), there is an 'opportunity springboard' to build tools that can predict the trajectories and spread of pathogens. Modelling has a key role to play in this journey.

Data availability

Daily reported case data for Aotearoa, New Zealand, are available from the Ministry of Health at https://github.com/minhealthnz/nz-covid-data[27] and 7-day average wastewater data are available from ESR at https://github.com/ESR-NZ/covid_in_wastewater[28]. The data used in this paper are also archived at https://doi.org/10.5281/zenodo.11081779[51].

Code availability

Code to run the model and reproduce the results in this paper are available at https://github.com/nicsteyn2/NZWastewaterModelling[29] and archived at https://doi.org/10.5281/zenodo.11081779[51].

Received: 22 August 2023; Accepted: 4 July 2024;
Published online: 15 July 2024

References

1. Colman, E., Puspitarani, G. A., Enright, J. & Kao, R. R. Ascertainment rate of SARS-CoV-2 infections from healthcare and community testing in the UK. *J. Theor. Biol.* **558**, 111333 (2023).
2. Eales, O. et al. Dynamics of SARS-CoV-2 infection hospitalisation and infection fatality ratios over 23 months in England. *PLoS Biol.* **21**, e3002118 (2023).
3. Vattiatio, G., Lustig, A., Maclaren, O. J. & Plank, M. J. Modelling the dynamics of infection, waning of immunity and re-infection with the Omicron variant of SARS-CoV-2 in Aotearoa New Zealand. *Epidemics* **41**, 100657 (2022).
4. Parag, K. V., Donnelly, C. A. & Zarebski, A. E. Quantifying the information in noisy epidemic curves. *Nat. Comput. Sci.* **2**, 584–594 (2022).
5. Dawood, F. S. et al. Incidence rates, household infection risk, and clinical characteristics of SARS-CoV-2 infection among children and adults in Utah and New York City, New York. *JAMA Pediatrics* **176**, 59–67 (2022).
6. Elliott, P. et al. Real-time assessment of community transmission (REACT) of SARS-CoV-2 virus: study protocol. *Wellcome Open Res.* **5**, 200 (2020).
7. Pouwels, K. B. et al. Community prevalence of SARS-CoV-2 in England from april to november, 2020: results from the ONS coronavirus infection survey. *Lancet Public Health* **6**, e30–e38 (2021).
8. Daughton, C. G. Wastewater surveillance for population-wide Covid-19: the present and future. *Sci. Total Environ.* **736**, 139631 (2020).
9. Dutta, H., Kaushik, G. & Dutta, V. Wastewater-based epidemiology: a new frontier for tracking environmental persistence and community transmission of COVID-19. *Environ. Sci. Pollut. Res.* **29**, 85688–85699 (2022).
10. Keshaviah, A. et al. Wastewater monitoring can anchor global disease surveillance systems. *Lancet Glob. Health* **11**, e976–e981 (2023).
11. Nourbakhsh, S. et al. A wastewater-based epidemic model for SARS-CoV-2 with application to three Canadian cities. *Epidemics* **39**, 100560 (2022).
12. Huisman, J. S. et al. Estimation and worldwide monitoring of the effective reproductive number of SARS-CoV-2. *eLife* **11**, e71345 (2022).
13. Huisman, J. S. et al. Wastewater-based estimation of the effective reproductive number of SARS-CoV-2. *Environ. Health Perspect.* **130**, 57011 (2022).
14. Asadi, M. et al. A wastewater-based risk index for SARS-CoV-2 infections among three cities on the Canadian prairie. *Sci. Total Environ.* **876**, 162800 (2023).
15. Wannigama, D. L. et al. COVID-19 monitoring with sparse sampling of sewered and non-sewered wastewater in urban and rural communities. *iScience* **26**, 107019 (2023).
16. Scire, J. et al. estimateR: An R package to estimate and monitor the effective reproductive number. *BMC Bioinformatics* **24**, 310 (2023).
17. Jiang, G. et al. Artificial neural network-based estimation of COVID-19 case numbers and effective reproduction rate using wastewater-based epidemiology. *Water Res.* **218**, 118451 (2022).
18. Pell, B., Brozak, S., Phan, T., Wu, F. & Kuang, Y. The emergence of a virus variant: dynamics of a competition model with cross-immunity time-delay validated by wastewater surveillance data for COVID-19. *J. Math. Biol.* **86**, 63 (2023).
19. Kisand, V. et al. Prediction of COVID-19 positive cases, a nation-wide SARS-CoV-2 wastewater-based epidemiology study. *Water Res.* **231**, 119617 (2023).
20. Geubbels, E. L. P. E. et al. The daily updated Dutch national database on COVID-19 epidemiology, vaccination and sewage surveillance. *Sci. Data* **10**, 469 (2023).
21. Cori, A., Ferguson, N. M., Fraser, C. & Cauchemez, S. A new framework and software to estimate time-varying reproduction numbers during epidemics. *Am. J. Epidemiol.* **178**, 1505–1512 (2013).
22. Thompson, R. N. et al. Improved inference of time-varying reproduction numbers during infectious disease outbreaks. *Epidemics* **29**, 100356 (2019).
23. Abbott, S. et al. Estimating the time-varying reproduction number of SARS-CoV-2 using national and subnational case counts. *Wellcome Open Res.* **5**, 112 (2020).
24. Fang, Z. et al. Wastewater monitoring of COVID-19: a perspective from Scotland. *J. Water Health* **20**, 1688–1700 (2022).
25. McManus, O. et al. Predicting COVID-19 incidence using wastewater surveillance data, Denmark, October 2021–June 2022. *Emerg. Infect. Dis.* **29**, 1589 (2023).
26. Bertels, X. et al. Time series modelling for wastewater-based epidemiology of COVID-19: a nationwide study in 40 wastewater treatment plants of Belgium, February 2021 to June 2022. *Sci. Total Environ.* **899**, 165603 (2023).
27. Ministry of Health. COVID-19 data for New Zealand. https://github.com/minhealthnz/nz-covid-data (2023).
28. ESR. COVID-19 data repository by the Institute of Environmental Science and Research. https://github.com/ESR-NZ/covid_in_wastewater (2023).
29. Watson, L. M. et al. NZ Wastewater Modelling Code. https://github.com/nicsteyn2/NZWastewaterModelling (2024).
30. Golding, N. et al. A modelling approach to estimate the transmissibility of SARS-CoV 2 during periods of high, low, and zero case incidence. *eLife* **12**, e78089 (2023).
31. Medema, G., Been, F., Heijnen, L. & Petterson, S. Implementation of environmental surveillance for SARS-CoV-2 virus to support public health decisions: opportunities and challenges. *Curr. Opin. Environ. Sci. Health* **17**, 49–71 (2020).
32. Nauta, M. et al. Early detection of local sars-cov-2 outbreaks by wastewater surveillance: a feasibility study. *Epidemiol. Infect.* **151**, e28 (2023).
33. Lustig, A. et al. Modelling the impact of the Omicron BA.5 subvariant in New Zealand. *J. R. Soc. Interface* **20**, 20220698 (2023).
34. Backer, J. A. et al. Shorter serial intervals in SARS-CoV-2 cases with Omicron BA.1 variant compared with Delta variant, the Netherlands, 13 to 26 December 2021. *Eurosurveillance* **27**, 2200042 (2022).
35. Hewitt, J. et al. Sensitivity of wastewater-based epidemiology for detection of SARS-CoV-2 RNA in a low prevalence setting. *Water Res.* **211**, 118032 (2022).
36. Gordon, N. J., Salmond, D. J. & Smith, A. F. M. Novel approach to nonlinear/non-gaussian Bayesian state estimation. *IEE Proc. F Radar Signal Process.* **140**, 107–113 (1993).

37. Douglas, J. et al. Tracing the international arrivals of SARS-CoV-2 Omicron variants after Aotearoa New Zealand reopened its border. *Nat. Commun.* **13**, 6484 (2022).
38. Kilaru, P. et al. Wastewater surveillance for infectious disease: a systematic review. *Am. J. Epidemiol.* **192**, 305–322 (2023).
39. Bunce, M., Geoghegan, J. L., Winter, D., de Ligt, J. & Wiles, S. Exploring the depth and breadth of the genomics toolbox during the COVID-19 pandemic: insights from Aotearoa New Zealand. *BMC Med.* **21**, 1–8 (2023).
40. Toribio-Avedillo, D. et al. Monitoring influenza and respiratory syncytial virus in wastewater. Beyond COVID-19. *Sci. Total Environ.* **892**, 164495 (2023).
41. Prasek, S. M. et al. Variant-specific SARS-CoV-2 shedding rates in wastewater. *Sci. Total Environ.* **857**, 159165 (2023).
42. Steyn, N. et al. Māori and Pacific people in New Zealand have a higher risk of hospitalisation for COVID-19. *N Z Med. J.* **134**, 1538 (2021).
43. Riley, S. et al. Resurgence of SARS-CoV-2: detection by community viral surveillance. *Science* **372**, 990–995 (2021).
44. Huang, Q. S. et al. Impact of the COVID-19 nonpharmaceutical interventions on influenza and other respiratory viral infections in New Zealand. *Nat. Commun.* **12**, 1001 (2021).
45. Zambon, M. C., Stockton, J. D., Clewley, J. P. & Fleming, D. M. Contribution of influenza and respiratory syncytial virus to community cases of influenza-like illness: an observational study. *Lancet* **358**, 1410–1416 (2001).
46. Eales, O. et al. Key challenges for respiratory virus surveillance while transitioning out of acute phase of COVID-19 pandemic. *Emerg. Infect. Dis.* **30**, e230768 (2024).
47. Schenk, H. et al. Prediction of hospitalisations based on wastewater-based SARS-CoV-2 epidemiology. *Sci. Total Environ.* **873**, 162149 (2023).
48. Brockhaus, E. K. et al. Why are different estimates of the effective reproductive number so different? A case study on COVID-19 in Germany. *PLoS Comput. Biol.* **19**, e1011653 (2023).
49. Plank, M. J., Watson, L. & Maclaren, O. J. Near-term forecasting of Covid-19 cases and hospitalisations in Aotearoa New Zealand. *PLoS Comput. Biol.* **20**, e1011752 (2024).
50. Moss, R., Zarebski, A., Dawson, P. & McCaw, J. M. Retrospective forecasting of the 2010-2014 Melbourne influenza seasons using multiple surveillance systems. *Epidemiol. Infect.* **145**, 156–169 (2017).
51. Watson, L. M. et al. NZ Wastewater Modelling Code. https://doi.org/10.5281/zenodo.11081779 (2024).
52. Abbott, S., Sherratt, K., Gerstung, M. & Funk, S. Estimation of the test to test distribution as a proxy for generation interval distribution for the Omicron variant in England. Preprint at *medRxiv* https://doi.org/10.1101/2022.01.08.22268920 (2022).
53. Kim, D. et al. Estimation of serial interval and reproduction number to quantify the transmissibility of SARS-CoV-2 Omicron variant in South Korea. *Viruses* **14**, 533 (2022).
54. Stats NZ. National population estimates: at 31 December 2022. https://www.stats.govt.nz/information-releases/national-population-estimates-at-31-december-2022/ (2023).

Acknowledgements

The authors acknowledge the role of the New Zealand Ministry of Health in supplying data in support of this work. The authors thank the wastewater treatment plant staff members who collected the wastewater samples and the ESR laboratory staff who processed and tested the samples used in this study. This work was funded by the New Zealand Ministry of Health and the Department of Prime Minister and Cabinet (DPMC). This work was supported by the NIHR HPRU in Emerging and Zoonotic Infections, a partnership between PHE, the University of Oxford, the University of Liverpool, and the Liverpool School of Tropical Medicine (grant number NIHR200907 supporting C.A.D.). L.M.W. was supported by a Rutherford Foundation Postdoctoral Fellowship from New Zealand government funding, administered by the Royal Society Te Apārangi. N.S. acknowledges support from the Oxford-Radcliffe Scholarship from University College, Oxford, and the Engineering and Physical Sciences Research Council (EPSRC) Centre for Doctoral Training (CDT) in Modern Statistics and Statistical Machine Learning (Imperial College London and University of Oxford). We thank A. Maslov for supporting this research through studentship support for N.S.

Author contributions

L.M.W.: conceptualisation, methodology, software, validation, investigation, writing—original draft, writing— review and editing, visualisation, and supervision. MJ.P.: conceptualisation, methodology, software, validation, investigation, writing—original draft, writing—review & editing, visualisation, and supervision. B.A.A.: investigation, data curation, resources, writing—review & editing. J.R.C: investigation, data curation, resources, writing—review & editing. J.H.: investigation, data curation, resources, writing—review & editing. H.M.: investigation, data curation, resources, writing—review & editing. A.O.: project administration, funding acquisition, writing—review & editing. M.B.: conceptualisation, project administration, funding acquisition, writing—review & editing. C.A.D.: conceptualisation, methodology, writing—review & editing. N.S.: conceptualisation, methodology, software, validation, investigation, writing—original draft, writing—review & editing, visualisation, and supervision.

Competing interests

The authors declare no competing interests.

Additional information

Supplementary information The online version contains supplementary material available at https://doi.org/10.1038/s43856-024-00570-3.

Correspondence and requests for materials should be addressed to Leighton M. Watson.

Peer review information *Communications Medicine* thanks David Larsen and the other, anonymous, reviewer(s) for their contribution to the peer review of this work.